analytical chemistry

pubs.acs.org/ac Article

In-Line Dopant Generation for Atmospheric Pressure Ionization Mass Spectrometry

G. Asher Newsome* and Timothy P. Cleland

Cite This: *Anal. Chem.* 2021, 93, 13527−13533 Read Online

ACCESS | Metrics & More | Article Recommendations | SI Supporting Information

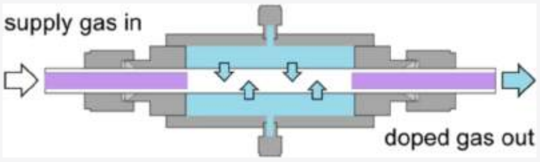

ABSTRACT: A concentric trace gas permeation tube that diffuses chemical reagents to a central carrier gas stream is used to drive chemical reaction pathways and influence gas-phase chemistry for a variety of atmospheric pressure ionization sources for mass spectrometry. Tunable permeation through the reservoir-jacketed polymer membrane is triggered by the heated gas moving through the tube, evaporating the dopant into a sheath dry gas or into a sample stream in room air without diluting the analyte concentration. The permeator is used to add dopants to an electrospray plume for analyte ion charge reduction and to perform hydrogen−deuterium exchange on biomolecules in different spray conditions. Dopants are also added to atmospheric pressure chemical ionization to favor the ionization of select components of diesel fuel. Atmospheric pressure photoionization is performed with the permeation tube in line with tubing transporting sample headspace to an enclosed discharge lamp. Toluene dopant from the permeator increases the proton transfer and charge exchange signal from clove oil and mothballs many times without exposing the laboratory to reagent fumes. Water permeation is also used to humidify the sample gas stream.

■ INTRODUCTION

Reliable generation of chemical vapors at atmospheric pressure is useful in many chemical and physical systems. Many of the most common and popular ionization techniques for mass spectrometry (MS) are performed at atmospheric pressure, including electrospray ionization (ESI), atmospheric pressure chemical ionization (APCI), atmospheric pressure photoionization (APPI), and all the variety of ambient ionization techniques that fundamentally operate on principles related to the former three. Whether the particular methodology necessarily requires an added reagent vapor to be efficient or advantageous,[1−3] the chemical environment in the atmosphere has positive and negative consequences for the analyte signal.[4,5] Most commercialized ion sources have enclosures and dry gases to shield from dynamic ambient conditions such as background variation or contamination[6] with limited effectiveness.[7]

Although it would be preferable to know the mass or concentration of dopant vapors, experimenters frequently settle for any generation method that can produce a chemical excess to drive a desired gas-phase reaction. Dopants are introduced to atmospheric pressure instrumentation either in a gaseous form or as a liquid to be volatilized. In MS applications, gas dopants are most frequently created through one of the following: passive evaporation directly from an open vessel[8,9] or enclosed container;[10] continuous infusion of a liquid to be evaporated at room temperature[11] or elevated temperatures;[12] bubbling through a liquid;[13,14] pressurizing headspace over a liquid;[15] liquid nebulization to produce a rapidly evaporating aerosol;[16,17] or with a supplemental electrospray.[18,19] Such systems are familiar to an experimentalist, may be enclosed or unenclosed, and are often easy to set up ad hoc. However, they may be unsuitable to or inconvenient for long-term use for a variety of reasons. Any un-enclosed or un-evacuated organic vapor generation is a safety hazard to laboratory occupants, and such a system creates tension between proper ventilation and the “hands-on” nature of much experimental work. Systems relying on evaporation at ambient temperatures are prone to poor reproducibility, but the addition of temperature and flow controls, nebulizers, and electrospray needles comes with greater complexity of multiple components. One system to add a dopant by bubbling through a solvent is commercialized but is limited to a particular electrospray source.[20] Dopant can be transmitted via a liquid chromatography eluent for that type of analysis but only if the reagent has no deleterious effects on separation hardware[2] and can serve the needs of both separation and ionization efficiency.[21]

Gas generation is not only more precise and operationally convenient but also more expensive with commercialized systems. Trace gas permeation tubes are liquid-containing capsules that, when heated in an oven, permeate reagents through their polymer walls[22] to evaporate into a carrier gas that is mixed with a zero gas.[23] The most abundant chemical in any atmospheric pressure system is water from ambient

Received: June 7, 2021
Accepted: September 20, 2021
Published: September 30, 2021

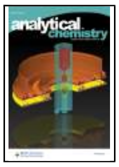

https://doi.org/10.1021/acs.analchem.1c02400
Anal. Chem. 2021, 93, 13527−13533

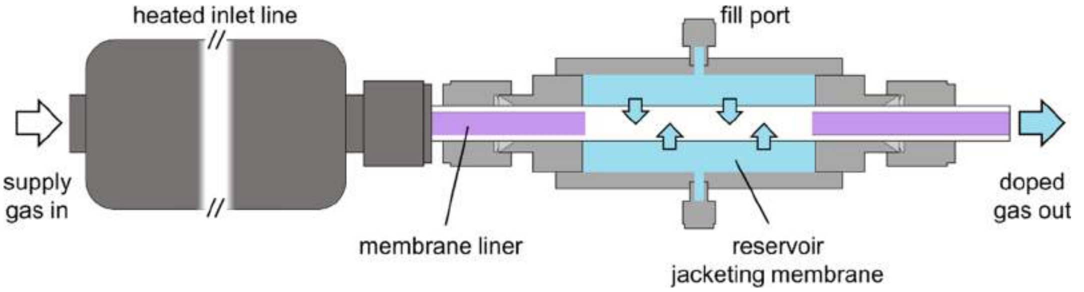

Figure 1. Heated inlet with a concentric permeation tube in cutaway view.

humidity, the level of which naturally varies. Accordingly, humidification is a common type of chemical addition, and commercial alternatives to passing carrier gas over saturated salt solutions[24] are water permeation tubes and heated-reservoir humidified air generators.[25] Regardless of the reagent or the means of generation, delivering a dopant in a sheath gas to mix with a gas-phase analyte for MS necessarily dilutes the analyte concentration in the added gas volume.

Miniaturization and multi-functionality of sampling and ion source components allow instrumentation to be operated in smaller spaces and with fewer parts, and perhaps no component is as universal to source design as tubing. Presented here is the use of a recently developed in-line trace gas permeator[26] to transport neutral, gas-phase molecules through a tube to an ionization source while adding a regulated amount of dopant to the gas stream. The gas generator is used as a compact device for reproducible, stand-alone operation peripheral to an ion source and as an integrated component of the sample transport system with ESI, APCI, and APPI systems. When atmospheric pressure tubing is used to transport neutral analyte molecules, the permeator outputs the dopant directly to the gas stream without diluting the analyte concentration or interrupting the laminar flow.

■ MATERIALS AND METHODS

Chemical reagents and analytes were obtained and used without further purification: acetone and bovine ubiquitin (Sigma-Aldrich, St. Louis, MO); acetonitrile, ammonium hydroxide, isopropanol, and toluene (Fisher Scientific, Hampton, NH); diethylamine (Beantown Chemical, Hudson, NH); methanol-[d_4] (D_3COD) (MilliporeSigma, Burlington, MA); human angiotensin I (Alfa Aesar, Haverhill, MA); and clove oil (Lorann Oils, Lansing, MI). 18 MΩ water was supplied by a Milli-Q filtration system (MilliporeSigma). Mothball and diesel fuel samples were obtained from retail. The dopant, analyte, and ion source usage is summarized in Table S1 (see the Supporting Information).

Dopant Generation. The permeation device consists of 6.4 mm o.d. and 4.7 mm i.d. polytetrafluoroethylene (PTFE) tubing sealed within a larger-diameter aluminum housing by stainless-steel ferrule-compression fittings at each end (Figure 1). Ports on the outer housing allow the liquid chemical reagent to be filled into the 2.3 mL space around the PTFE tubing within the housing. The liquid is pipetted into the reservoir through one fill port while air escapes the second port, and both are capped. To minimize any potential memory effects from volatile samples in PTFE,[27] stainless steel, 4.6 mm o.d. and 0.19 mm thick wall tubing liners coated with SilcoNert (SilcoTek, Bellefonte, PA) are inserted into each tubing end for at least the length of the end fittings. The PTFE is thus shielded from contact with gas and/or analyte flowing through the tube except in the reservoir-jacketed center. The maximum length of the reservoir-jacketed, unshielded membrane is 16.3 mm, which can be shielded further by pushing the coated insert liners inward.

A length of 6.4 mm o.d. heated inlet tubing (Clayborn Lab, Truckee, CA) was connected to the jacketed reservoir by fitting to the upstream end of the protruding PTFE tubing. Gas flow through the assembly was created by the positive pressure of ultrahigh-purity nitrogen applied to the heated inlet tubing, or by suction of room air from the downstream end of the permeator with a mass spectrometer inlet vacuum and/or a tunable diaphragm pump (Vacuubrand MZ2NT, Essex, CT). All gas flow rates were measured with a flow calibrator (Defender 510, Mesa Labs, Butler, NJ). Temperature settings up to 198 °C were maintained at +0/−2 °C relative to the setpoint on 1−2 m heated inlet tubing. Heated gas from the inlet warmed the exposed PTFE membrane, increasing the porosity and allowing the liquid from the reservoir to permeate through and evaporate into the gas stream. Multiple permeation devices with different dopants were swapped from the flow system as necessary between experiments. The device mass was measured with a triple-beam balance (720-T, Fisher Science, Hampton, NH) to the nearest 0.05 g. After use, the permeation device was allowed to return to room temperature and to retain the dopant in the reservoir. Permeation devices were also occasionally cleaned for reuse with different dopants in a fume hood by pouring out the remaining solvent, blowing through the reservoir with an inert gas, and drying.

Ionization and MS. ESI and APCI were performed in the IonMax source housing (Figure S1) on an LTQ Orbitrap Velos mass spectrometer (Thermo Fisher Scientific, Waltham, MA). The front-facing window of the IonMax was replaced with a sealed feed-through for a bulkhead fitting or by insertion of the entire permeator. The sheath or auxiliary nitrogen supplies were connected to the heated gas inlet and the permeation-doped outflow directed at the electrospray plume or corona needle in various ways.

For ESI, sample solutions were infused to a 3.5 kV HESI-II probe at a rate of 3 μL/min. The ESI needle was approximately 3 cm from the heated inlet. Peptide and protein samples were prepared at 5−10 μg/mL in 50:50 methanol/water with 0.1% formic acid for electrospray in denatured or non-native conditions and at 200 μg/mL in 50 mM ammonium acetate in water for electrospray in native conditions. Native-spray experiments required the sheath nitrogen flow to be set at 8 (arbitrary units), while doped or un-doped nitrogen flow was added through auxiliary nitrogen (Table S2).

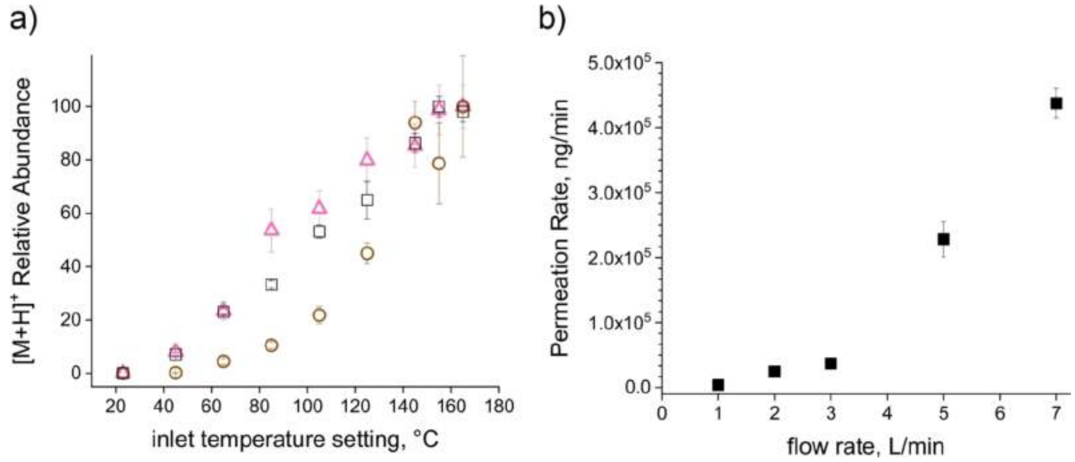

Figure 2. (a) APPI ion trap MS detection of isopropanol (black squares), acetone (brown circles), and acetonitrile (pink triangles) permeated into room air pulled through the in-line permeation tube and the heated inlet with various temperatures settings at 3.6 L/min, standard deviation error bars; (b) isopropanol permeation into room air flow through the tube connected to the 150 °C inlet, with standard deviation error bars for triplicate measurements at gas flow rates of 3 L/min and above.

A corona needle mounted in front of the mass spectrometer inlet from the corresponding IonMax port was discharged at 5−7 kV for APCI. The analyte headspace from bulk liquid samples was introduced from vessels mounted at the solvent waste port.

For APPI, the mass spectrometer was fitted with a Vapur inlet (IonSense, Saugus, MA) and a supplemental diaphragm pump. A 12.7 mm diameter krypton discharge lamp (Syagen Opton-20026) was independently mounted and connected to the Vapur with a stainless-steel ultra-torr tee fitting, sealed by the O-ring without ferrules and nuts (Figure S2). Sample vessels were mounted at the entrance to the heated inlet line, and the gas-phase analyte in room air was pulled through the line with the dopant added by the permeation device before the mixture enters the connection tee with the lamp.

MS analysis was performed with FT data acquired at 30,000 resolving power with a maximum ion trap fill time of 100 ms in either the profile or centroid mode, and ion trap scans in the low mass profile mode had a maximum fill time of 50 ms. Control experiments with the heated, un-doped gas were used to compare the analyte performance with the dopant.

■ RESULTS AND DISCUSSION

Permeation Rate. Trace gas generation systems with traditional permeation tubes and ovens use the ideal gas constant and a derived temperature dependence to calculate the concentration of reagents in the mixture of carrier gas and zero gas.[28,29] The in-line permeation system was likewise dependent on the carrier gas temperature (Figure 2a). Permeation of three volatile solvents appeared to plateau around a temperature setting of 150 °C for that particular inlet tubing and the flow rate without the ionization/detection efficiency being saturated. When the device was disconnected entirely, the signal dropped out immediately for all dopants discussed in this work. By permeating into a single air stream, the permeation rate was measured directly from mass loss from the reservoir over time (Figure 2b, low flow detail, Figure S3). Each rate measurement timed the loss of 0.65 up to 1.35 g of isopropanol from the reservoir, except for measurement at 1.0 L/min, which required over 2 weeks to permeate 0.10 g at a rate of 4000 ng/min. Rate measurements were acquired by connecting the room temperature permeator after the inlet was stably heated, thereby minimizing the warm up of the system relative to the total period. The ambient room air used as a carrier varied in humidity between the extremes of 1 and 10 g/m^3 absolute humidity through the months required to collect all rate measurements but also cycled through smaller ranges over 24 h periods. The change in the permeation rate with flow had two linear regions with an inflection point at 3.0 L/min. Higher flow rates carry heated air to the exposed PTFE membrane with less cooling in the ~8 cm fitting connecting the heated inlet, resulting in more efficient permeation. The heating mechanism places a practical upper limit on the length of the membrane, as the flowing gas would eventually cool too much to induce permeation. The heated inlet tubing is also eventually unable to maintain a temperature setpoint at sufficiently high flow rates of cool carrier gas entering the inlet. The observed permeation rates for the as-described device were comparable to the upper rates for traditional trace gas permeation tubes, that is, 1000 to hundreds of 1000 ng/min.

In addition to regulation by temperature and gas flow rate, the permeation rate could be adjusted by obscuring part of the membrane area with liner inserts. For expedience, the proof-of-principle was demonstrated at a high gas flow rate, and the permeation rate decreased linearly as the membrane was obscured (Figure S4). The full reservoir-jacketed membrane length is short enough to be unaffected by differential heating with increasing distance from the inlet. The trend has a positive *y* intercept because the pushed-in liner did not completely shield the obscured area from heat, and the permeated reagent could still reach the unshielded region. Slower gas flow rates that heat the membrane less efficiently might result in a trend that goes through the origin. Lower permeation rates would not typically be sought for trace gas use as a dopant, where the usual goal is an excess of reagent but could prove useful in experiments where the reagent amount is to be tuned.

Dopant Addition to Partly Enclosed ESI and APCI Sources. The permeation device was used as a stand-alone trace gas generator to add charge-reducing dopant to electrospray analytes. Similar to experiments in which organic solvents were added to the bulk analyte solution,[13] isopropanol vapor produced a modest shift in the charge state distribution

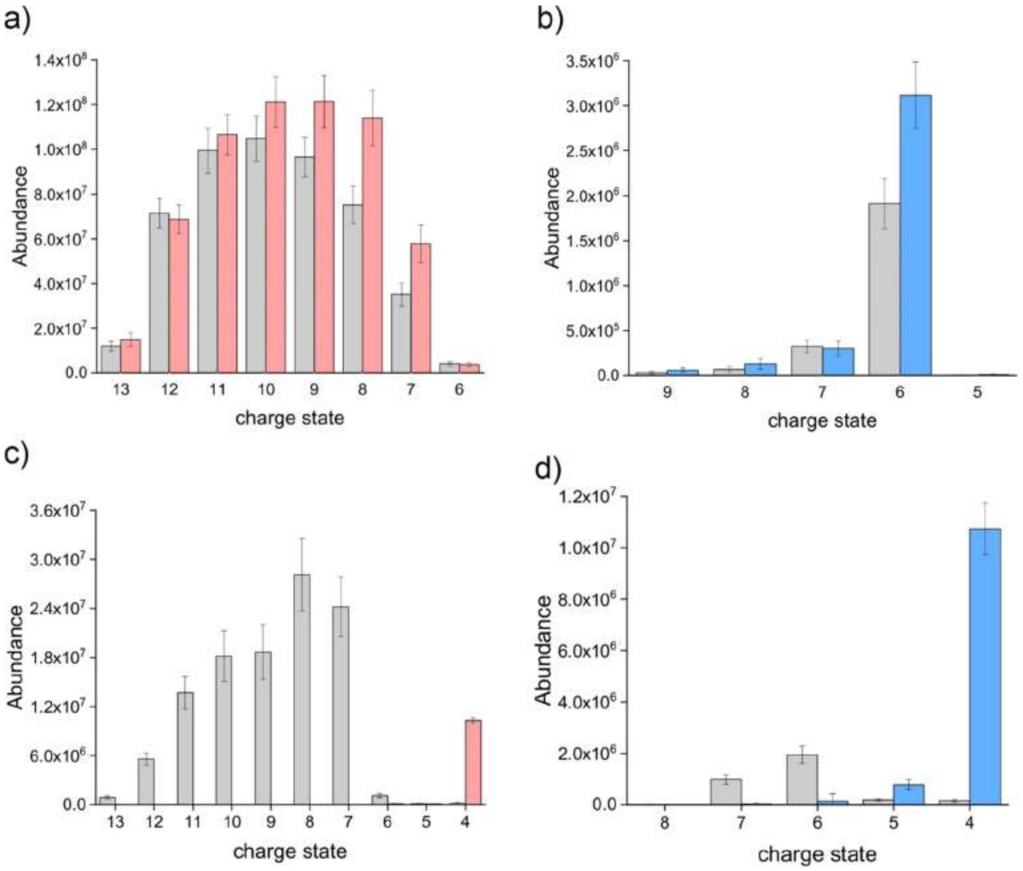

Figure 3. Summed isotope peak abundance from a denatured (a,c) and a native (b,d) ubiquitin electrospray plume exposed to un-doped nitrogen (gray columns) auxiliary gas at 3.5 L/min and auxiliary nitrogen doped (red/blue columns) with isopropanol (a,b) or diethylamine (c,d), with standard deviation error bars.

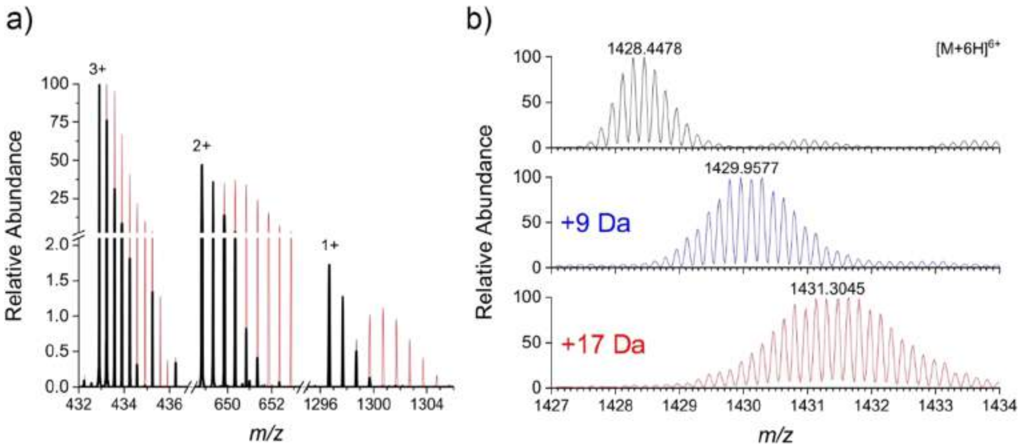

Figure 4. HDX of acidified electrospray plumes of (a) angiotensin I and (b) ubiquitin exposed to un-doped nitrogen auxiliary gas (black traces) at (a) 4.4 and (b) 3.5 L/min or auxiliary nitrogen doped with deuterated methanol (red traces). Native-spray ubiquitin was also exposed to auxiliary nitrogen doped with deuterated methanol (blue trace).

of ubiquitin toward lower charge and a small increase in intensity among the most abundant respective peaks (Figure 3a). The 10 most abundant isotope peaks within each charge state were summed for easy visual comparison of respective charge state abundances. Isopropanol added to ubiquitin in a native-spray solution produced no wholesale changes in the charge state but further shifted toward the +6 charge state for a 50% increase in signal intensity (Figure 3b). The vapor of the much more basic diethylamine had a substantially greater effect, condensing the denatured ubiquitin charge envelope into the +4 charge state (Figure 3c). The charge-reduced form had one-third abundance of the largest un-doped signal but 100 times un-doped +4 charge state abundance. For native-spray ubiquitin, the diethylamine vapor shifted the principle charge state from +6 to +4, as well as increased the signal abundance 5-fold (Figure 3d). Ubiquitin was previously charge-shifted only as low as +6 using an at least 10 times greater gas-phase concentration of the more basic dopant triethylamine.[30]

Hydrogen−deuterium exchange (HDX) experiments were performed for electrospray analytes by permeating deuterated methanol into nitrogen directed at the electrospray plume. Directly comparing signals for the monoisotopic single-charged ion, at least one deuterium exchange was observed for 98% of angiotensin I sprayed in an acidic solution (Figure 4a). The +1 form allowed HDX at all four rapid-exchange positions[31] for a 4 Da shift, the +2 form produced a 3 Da shift, and the +3 form produced a 1 Da shift. Differential HDX was observed for a given charge state of ubiquitin in either denatured or native-spray conditions (Figure 4b), producing more extensive exchange for the former. The unequal effect shows that the charge state cannot be equated with a single conformation and may also be influenced by different evaporation rates for microdroplets of different solvent makeup. HDX through the reaction between primary and supplemental electrospray microdroplets has been shown to be faster than the reaction in the bulk solution;[31] it may follow that the reaction between microdroplets and the gas-phase deuterated solvent is faster still if the experiment is repeated at a nanoscale. The observed exchange in native-spray conditions exposed to similar sheath gas flow rates was comparable to that of prior observations.[32] The number of observed deuterium exchanges decreased with the native-spray ubiquitin charge state to reflect the folding of the molecule, the +7 form producing a 10 Da shift, +6 form producing a 9 Da shift, and the +5 form producing an 8 Da shift. Both analytes in acidified solutions had deuterium exchange patterns relative to the charge state that were not primarily influenced by molecular folding. Denatured ubiquitin is large enough to show the mass shift increase and decrease with the charge state (Figure S5).

In addition to shifting the charge state distribution and the HDX of biomolecules, the stand-alone trace gas generator was used to modify the gas-phase chemistry for small-molecule analysis. APCI commonly uses a sheath gas flow in the housing containing the corona needle. Ammonia from decomposition of ammonium hydroxide was permeated into a heated nitrogen sheath. The basification of the bath gas decreased 10-fold the abundance of hydronium and the proton-bound water dimer (Figure S6), the usual proton-transfer reagent ions in APCI created from residual humidity in the semi-enclosed source housing. The altered reagent ion mixture was used to ionize compounds in diesel fuel fumes in comparison to un-doped nitrogen flow. While there was some ammoniation of hydrocarbons, the most significant effect was to shift the major peaks of the mass spectrum away from hydrocarbons to substituted phenols and other alcohol-containing compounds (Figure 5). The signal intensity of the latter was increased 10-fold as ammonia suppressed the hydrocarbon signal intensity proportionally. When the permeation device was used to introduce acetone, a reagent that favors proton transfer, the identities of major peaks of the mass spectrum were largely unchanged (Figure S7). Acetone significantly increased the overall abundance of intact ions because it has a higher proton affinity than water, leaving less energy after protonation available to cause analyte ion fragmentation.

Sample Transport and Dopant Addition to Enclosed APPI Source. APPI is typically performed without an enclosure or in a semi-enclosed source housing such as the IonMax. The shape of the lamp and the magnesium fluoride window made it possible to integrate into sample transport tubing.[33] The enclosure protected the ionization process from interference,[7] and excess dopant was safely evacuated by the instrument and supplemental vacuum system venting. The in-line permeation tube was used to add toluene dopant to the analyte headspace in room air conducted by the heated inlet, demonstrating both proton transfer and charge exchange ionization pathways. Although the pathways are competitive[3] and the amount of dopant generated by the tube may be lower than that from evaporation or nebulization of a bulk solvent, there is sufficient concentration for favorable proton transfer. The addition of toluene tripled the protonated molecule signal abundance observed from safrole ($[C_{10}H_{11}O_2]^+$) and other compounds in clove oil, compared to APPI using proton transfer from ambient humidity (Figure 6a). The proton-transfer signal from $[C_{25}H_{35}O_2]^+$ increased closer to 10-fold. Signal abundance was also tripled for naphthalene ($[C_{10}H_8]^{+\bullet}$) from mothballs, which was ionized through charge exchange (Figure 6b). Toluene did not appreciably change the signal abundance of proton-transfer background ions such as $[C_{24}H_{38}O_4]^+$ from phthalates in the laboratory air that have a higher proton affinity.

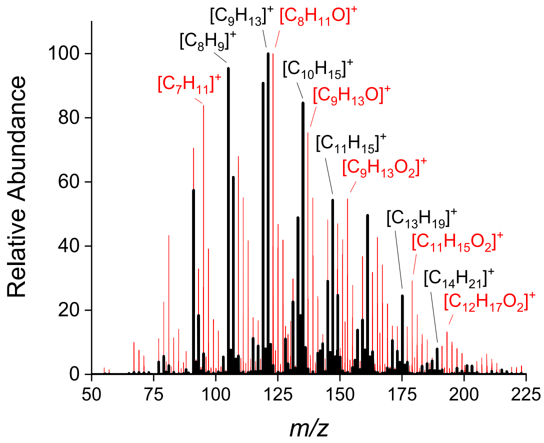

Figure 5. APCI of the diesel headspace exposed to the un-doped nitrogen auxiliary gas at 4.9 L/min (black trace) and auxiliary nitrogen doped with ammonia (red trace).

Humidity Regulation. Analyte spectra have been shown to be affected by ambient humidity, which can be tracked mass spectrometrically by the abundance of the proton-bound water dimer.[25] Addition of water vapor to relatively dry ambient room air through the concentric permeation tube likewise increased water dimer abundance in APPI spectra without other dopants (Figure 7). Humidification was also measured directly with a hygrometer probe sealed in place of the APPI lamp (Figure S8), which measured a similar dependence on the inlet temperature. Together, the results show that the permeation device can raise the incoming room air transporting gas-phase analyte to a particular humidity level before ionization. The phthalate fragmentation change indicates the significance of humidity for the proton-transfer ion signal.

■ CONCLUSIONS

Demonstrating its wide experimental applicability, the in-line gas permeation tube was used as a stand-alone dopant generator to influence analyte ionization from multiple sources without instrumental modification other than redirecting nitrogen from the ion source housing supply. Permeated reagents for the various ion sources ranged in volatility above

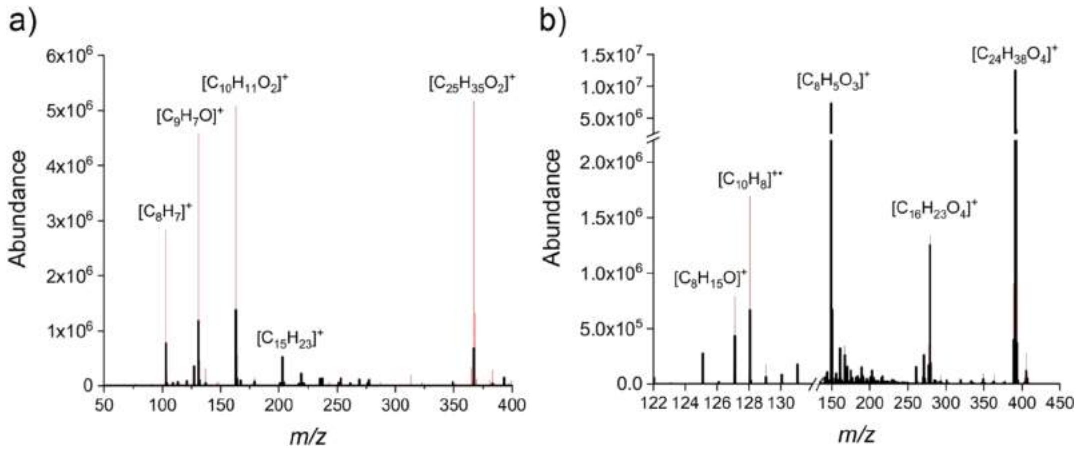

Figure 6. APPI of (a) background-subtracted clove oil or (b) mothball headspace in room air pulled through the inlet at (a) 6.0 L/min or (b) 5.3 L/min (black trace) and air doped with toluene (red trace).

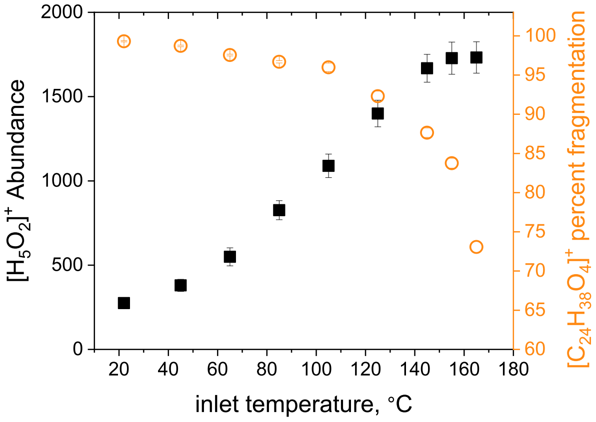

Figure 7. Mass spectral abundance of water dimer (black squares) and percent fragmentation of background phthalate (orange circles) from APPI of room air originally at 2.8 g/m^3 absolute humidity (13.8% relative humidity, 22.7 °C) after being pulled through the water permeation tube and inlet of various temperatures at 3.6 L/min, with standard deviation error bars.

and below that of water. Charge reduction and deuteration of electrosprayed biomolecules were notably as extensive as or more extensive than similar respective experiments using gas-phase reagents and microdroplets. Future experiments will also demonstrate the performance of the permeation device with post-column additives to nano-flow ESI. The device offers a convenient but reproducible means of enforcing ionization pathways for APCI with corona discharge and other techniques that induce proton transfer and/or charge exchange. By putting the permeator in series with sample inlet tubing and a sealed-in discharge lamp, APPI experiments demonstrated the dual functionality of the device for sample transport and dopant addition without dilution. No other configuration for APPI has so enclosed the dopant source to eliminate laboratory exposure, and the design could safely accommodate more noxious reagents than those tested here without risk to the analyst. The gas generator also offers the ability to add a reproducible amount of water vapor to the analyte in room air prior to in-line ionization, accounting for the variance of ambient humidity.

The simplicity of the in-line permeation device design confers practical operational advantages to various analytical and MS operations. As a small, jacketed tube with pipe terminals, the permeator was easy to position and attach/detach with conventional fittings. The inexpensive design allowed the use of multiple permeators with different solvents to be quickly swapped into and out of the system. The heated inlet tubing used to drive permeation is both commercially available and commonly home-built. The unit described needs only a small reservoir to accommodate its low permeation rates, and the reservoir is refillable, reusable with different solvents, and would accommodate a supplemental reservoir attachment to allow permeation to continue indefinitely. Like all permeation tubes, the device was subject to an activation time of some minutes to arrive at the requisite temperature and dispense the dopant at a steady rate. Once stabilized, the dopant permeation rate was predictable and reproducible, while the design was flexible for use at different gas flow rates. Like commercial permeation systems which calibrate for each trace gas, further gravimetric permeation rate measurements with other solvents can confirm the universality of permeation response. In addition to temperature and gas flow rate control, the permeation rate was lowered by reducing the membrane area exposure, which might be useful for applications that use low dopant concentrations.[34] As the dimensionality of the polymer membrane is the only factor limiting the functionality, the design might be reproduced in various sizes for various analytical applications, even increasing the permeation rate by reducing the membrane thickness.

■ ASSOCIATED CONTENT

Supporting Information

The Supporting Information is available free of charge at https://pubs.acs.org/doi/10.1021/acs.analchem.1c02400.

> Dopants and ion sources used throughout; IonMax source housing configuration; actual nitrogen flow rates for HESI source settings; configuration of the APPI lamp and the sampling system; permeation at low flow rates; permeation with liners over the membrane surface; HDX mass shifts for denatured ubiquitin; APCI of the ammonia dopant; APCI of diesel with acetone; and hygrometer measurement of in-line permeated humidity (PDF)

AUTHOR INFORMATION

Corresponding Author

G. Asher Newsome – *Smithsonian Museum Conservation Institute, Suitland, Maryland 20746, United States;* orcid.org/0000-0003-1683-2197; Phone: 301-238-1223; Email: newsomeg@si.edu; Fax: 301-238-3709

Author

Timothy P. Cleland – *Smithsonian Museum Conservation Institute, Suitland, Maryland 20746, United States;* orcid.org/0000-0001-9198-2828

Complete contact information is available at: https://pubs.acs.org/10.1021/acs.analchem.1c02400

Notes

The authors declare no competing financial interest.

ACKNOWLEDGMENTS

The authors thank Eloy Wouters of Thermo Scientific for initial loaning of the APPI lamp and Michael Malito of the US Naval Research Laboratory for fabricating the IonMax feedthrough. This project was generously supported by the Smithsonian Scholarly Studies Award and the Smithsonian's Museum Conservation Institute Federal Funds.

REFERENCES

(1) Kauppila, T. J.; Kuuranne, T.; Meurer, E. C.; Eberlin, M. N.; Kotiaho, T.; Kostiainen, R. *Anal. Chem.* **2002**, *74*, 5470–5479.

(2) Hahne, H.; Pachl, F.; Ruprecht, B.; Maier, S. K.; Klaeger, S.; Helm, D.; Médard, G.; Wilm, M.; Lemeer, S.; Kuster, B. *Nat. Methods* **2013**, *10*, 989–991.

(3) Vaikkinen, A.; Kauppila, T. J.; Kostiainen, R. *J. Am. Soc. Mass Spectrom.* **2016**, *27*, 1291–1300.

(4) Song, L.; Gibson, S. C.; Bhandari, D.; Cook, K. D.; Bartmess, J. E. *Anal. Chem.* **2009**, *81*, 10080–10088.

(5) Newsome, G. A.; Ackerman, L. K.; Johnson, K. J. *Anal. Chem.* **2014**, *86*, 11977–11980.

(6) Nugent, K.; Zhu, Y.; Kent, P.; Phinney, B.; Alvarado, R. CaptiveSpray: A New Ionization Technique to Maximizing Speed, Sensitivity, Resolution and Robustness for LCMS Protein Biomarker Quantitation. *57th ASMS Conference on Mass Spectrometry and Allied Topics*, Philadelphia, PA, 2009.

(7) Strmeň, T.; Vrkoslav, V.; Bosakova, Z.; Cvacka, J. *Rapid Commun. Mass Spectrom.* **2020**, *34*, No. e8722.

(8) Hopper, J. T. S.; Sokratous, K.; Oldham, N. J. *Anal. Biochem.* **2012**, *421*, 788–790.

(9) Banerjee, S. *J. Mass Spectrom.* **2013**, *48*, 193–204.

(10) Javanshad, R.; Maser, T. L.; Honarvar, E.; Venter, A. R. *J. Am. Soc. Mass Spectrom.* **2019**, *30*, 2571–2575.

(11) Jorabchi, K.; Hanold, K.; Syage, J. *Anal. Bioanal. Chem.* **2013**, *405*, 7011–7018.

(12) Dwivedi, P.; Wu, C.; Matz, L. M.; Clowers, B. H.; Siems, W. F.; Hill, H. H. *Anal. Chem.* **2006**, *78*, 8200–8206.

(13) Iavarone, A. T.; Jurchen, J. C.; Williams, E. R. *J. Am. Soc. Mass Spectrom.* **2000**, *11*, 976–985.

(14) Liu, C.; Yang, J.; Wang, J.; Hu, Y.; Zhao, W.; Zhou, Z.; Qi, F.; Pan, Y. *J. Am. Soc. Mass Spectrom.* **2016**, *27*, 1597–1605.

(15) McCulloch, R. D.; Robb, D. B.; Blades, M. W. *Rapid Commun. Mass Spectrom.* **2008**, *22*, 3549–3554.

(16) Robb, D. B.; Covey, T. R.; Bruins, A. P. *Anal. Chem.* **2000**, *72*, 3653–3659.

(17) Kauppila, T. J.; Östman, P.; Marttila, S.; Ketola, R. A.; Kotiaho, T.; Franssila, S.; Kostiainen, R. *Anal. Chem.* **2004**, *76*, 6797–6801.

(18) Mark, L. P.; Gill, M. C.; Mahut, M.; Derrick, P. J. *Eur. J. Mass Spectrom.* **2012**, *18*, 439–446.

(19) Zheng, Z.; Attygalle, A. B. *J. Am. Soc. Mass Spectrom.* **2021**, *32*, 725–735.

(20) Bruker Daltonik GmbH. CaptiveSpray nanoBooster—The Revolution in Proteomics Ionization. https://www.bruker.com/products/mass-spectrometry-and-separations/lc-ms/ion-sources/captivespray-nanobooster/overview.html (accessed 2020).

(21) Kostiainen, R.; Kauppila, T. J. *J. Chromatogr. A* **2009**, *1216*, 685–699.

(22) Mckinley, J. J., Jr. Gas Detection Apparatus. U.S. Patent 3,438,241 A, 1969.

(23) McKinley, J. *Gases Instrum.* **2008**, 2 (1), 22–26.

(24) Rockland, L. B. *Anal. Chem.* **1960**, *32*, 1375–1376.

(25) Newsome, G. A.; Ackerman, L. K.; Johnson, K. J. *J. Am. Soc. Mass Spectrom.* **2016**, *27*, 135–143.

(26) Newsome, G. A.; Malito, M. P.; Johnson, K. J. Concentric Permeation System for Transfer of Neutral Gaseous Material. U.S. Patent 20210296107 A1, 2021.

(27) Usmanov, D. T.; Hiraoka, K.; Wada, H.; Matsumura, M.; Sanada-Morimura, S.; Nonami, H.; Yamabe, S. *Anal. Chim. Acta* **2017**, *973*, 59–67.

(28) Interscan Corporation. Perm tube tech: Rigorous discussion of "*K*" value and best way to calculate gas concentration. https://www.gasdetection.com/gas-detection-knowledge-base/calibration-issues/rigorous-discussion-of-k-value-and-best-way-to-calculate-gas-concentration/ (accessed 2021).

(29) Boyle, B. Generating Calibration Gas Standards with OVG-4 and Permeation Tubes. https://www.gasdetection.com/wp-content/uploads/Whitepaper_-_Generating_Calibration_Gas_Standards_with_OVG-4_and_Permeation_Tubes.pdf (accessed 2021).

(30) Ogorzalek Loo, R. R.; Smith, R. D. *J. Am. Soc. Mass Spectrom.* **1994**, *5*, 207–220.

(31) Jansson, E. T.; Lai, Y.-H.; Santiago, J. G.; Zare, R. N. *J. Am. Chem. Soc.* **2017**, *139*, 6851–6854.

(32) Sanguantrakun, N.; Chanthamontri, C.; Gross, M. L. *J. Am. Soc. Mass Spectrom.* **2020**, *31*, 1151–1154.

(33) Haapala, M.; Teppo, J.; Ollikainen, E.; Kiiski, I.; Vaikkinen, A.; Kauppila, T. J.; Kostiainen, R. *Anal. Chem.* **2015**, *87*, 3280–3285.

(34) Liu, H.; Xia, L.; Shen, C.; Huang, C.; Chu, Y. *Anal. Bioanal. Chem.* **2021**, *413*, 4237–4246.

Supporting Information

In-line Dopant Generation for Atmospheric Pressure Ionization Mass Spectrometry

G. Asher Newsome*, Timothy P. Cleland
Smithsonian Museum Conservation Institute, Suitland, Maryland, 20746
Phone: 301-238-1223
Fax: 301-238-3709

**to whom correspondence may be addressed*: newsomeg@si.edu

Table of Contents

Table S1. Dopants and ion sources used with mass spectrometry to study analytes.

dopant	ion source	analyte	Figure
isopropanol	ESI	ubiquitin (denatured), ubiquitin (native)	3a, 3b
diethylamine	ESI	ubiquitin (denatured), ubiquitin (native)	3c, 3d
methanol-[D_4]	ESI	angiotensin I, ubiquitin (denatured and native)	4a, 4b
ammonia	APCI	diesel	5
acetone	APCI	diesel	S5
isopropanol	APPI	isopropanol	2a
acetone	APPI	acetone	2a
acetonitrile	APPI	acetonitrile	2a
toluene	APPI	clove oil, mothballs	6a, 6b
water	APPI	water dimer, phthalate background	7

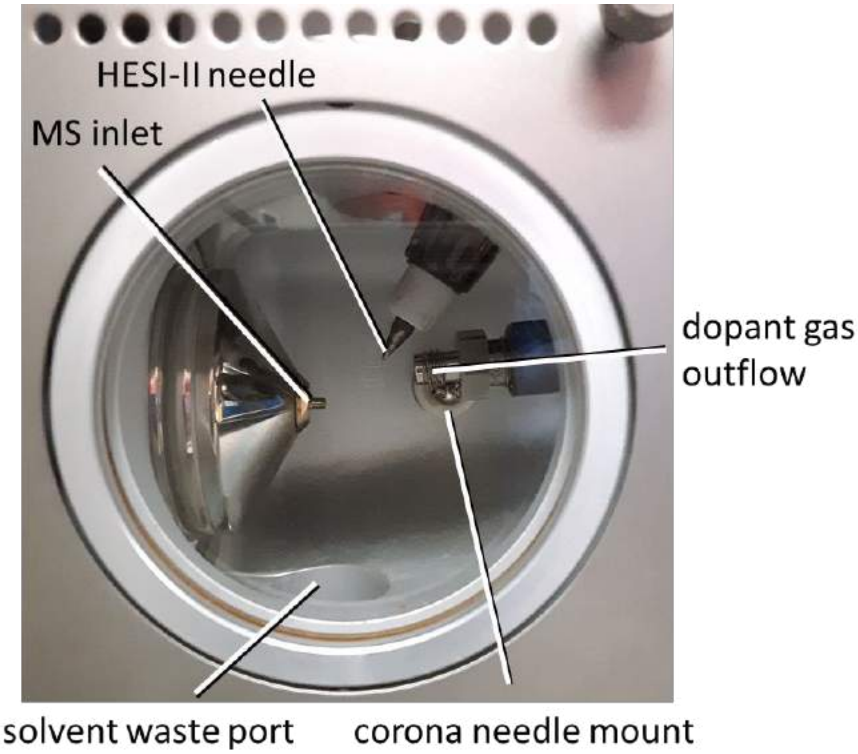

Figure S1. IonMax source housing configuration (corona needle absent).

Table S2. Actual nitrogen flow rates from arbitrary settings for HESI source.

sheath nitrogen (arbitrary)	auxiliary nitrogen (arbitrary)	measured flow rate, L/min
	3	3.49
3		4.35
	5	4.85
5		5.96
	8	6.51
8		8.05
	10	7.52
10		9.30

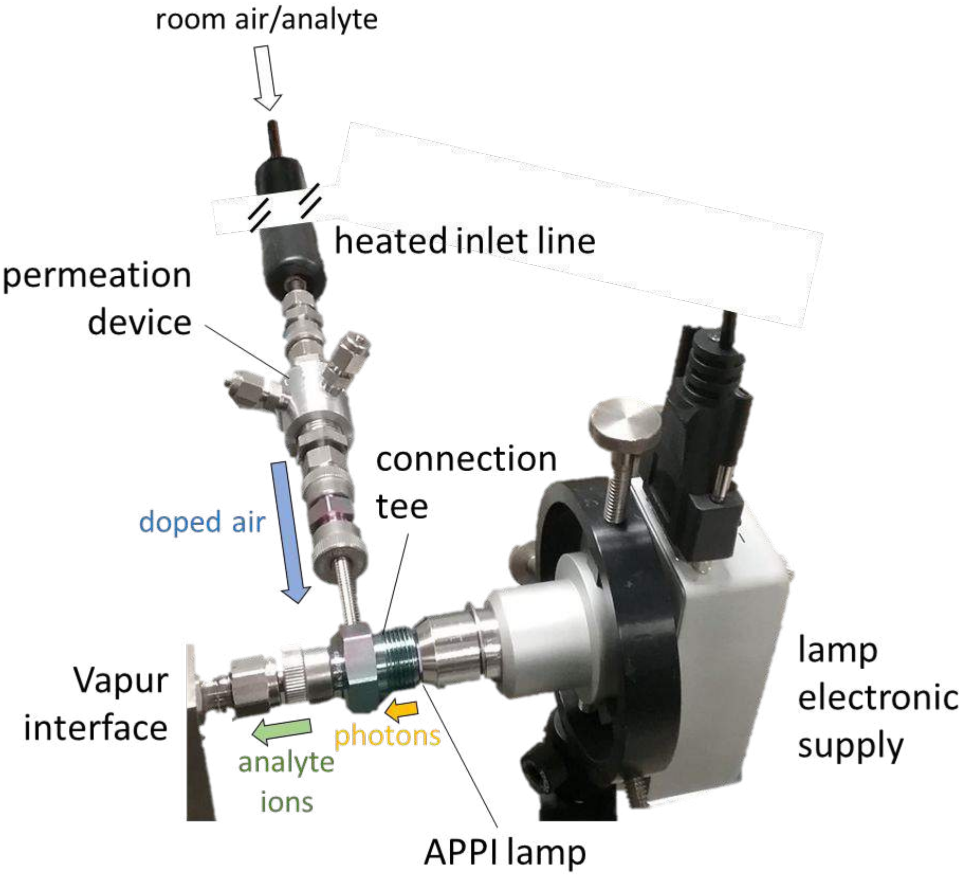

Figure S2. APPI lamp connected to dopant permeation/sampling line and Vapur interface on LTQ Orbitrap Velos.

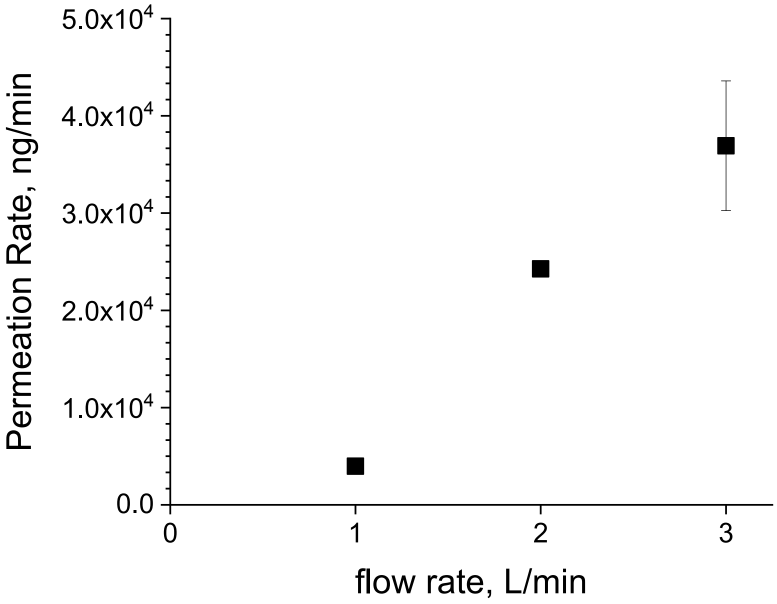

Figure S3. Detail from Figure 2, isopropanol permeation into room air flow through tube connected to 150 °C inlet, with standard deviation error bars for triplicate measurements at 3 L/min.

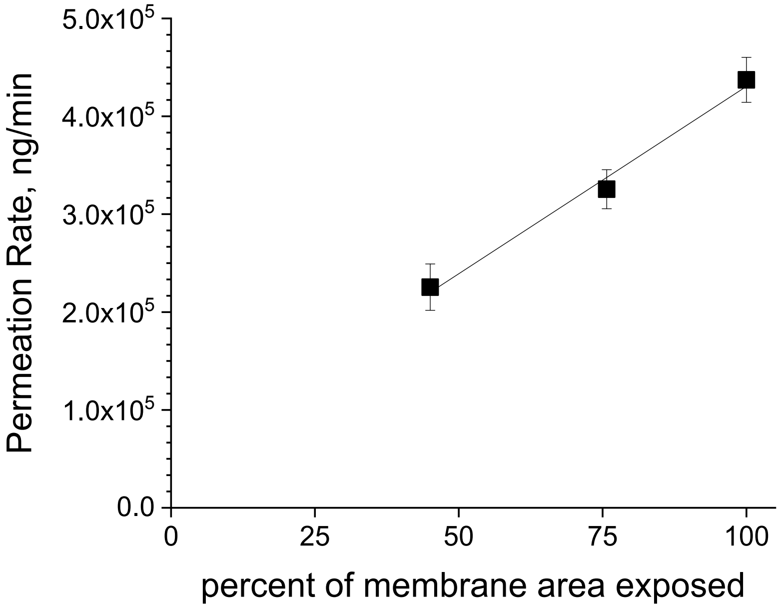

Figure S4. Isopropanol permeation with the upstream insert liner covering different portions of the membrane surface, 7.0 L/min room air flow through tube connected to 150 °C inlet, standard deviation error bars.

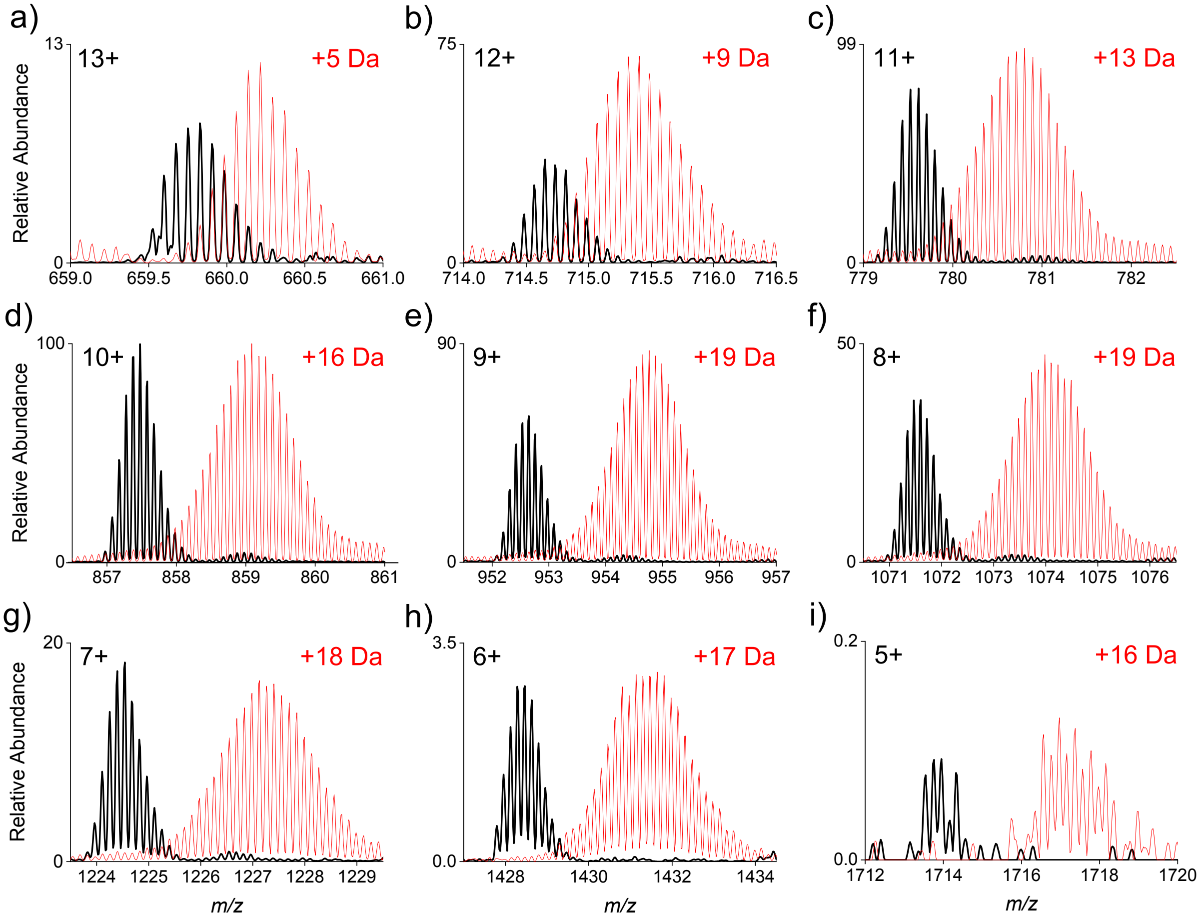

Figure S5. Mass shifts from denatured ubiquitin electrospray (black traces) exposure to 3.5 L/min of auxiliary nitrogen doped with deuterated methanol (red traces), charge states a) 13+, b) 12+, c) 11+, d) 10+, e) 9+, f) 8+, g) 7+, h) 6+, i) 5+.

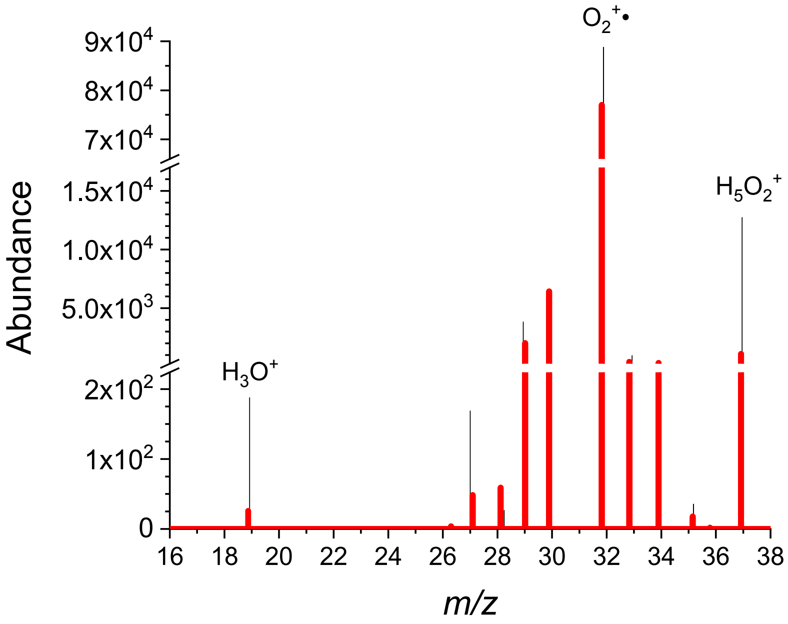

Figure S6. APCI of un-doped nitrogen auxiliary gas at 4.9 L/min (black trace); and auxiliary nitrogen doped with ammonia (red trace).

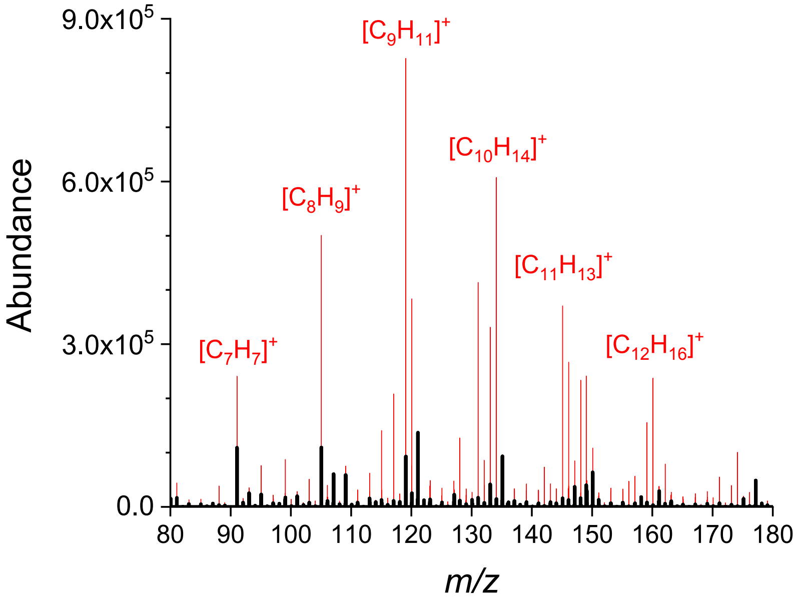

Figure S7. APCI of diesel headspace exposed to un-doped nitrogen auxiliary gas at 4.9 L/min (black trace); and auxiliary nitrogen doped with acetone (red trace).

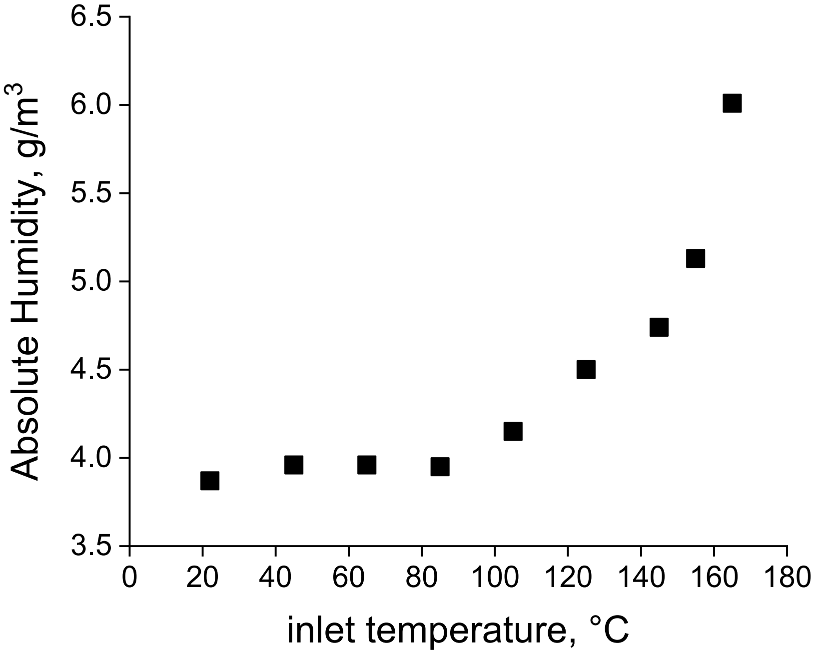

Figure S8. Hygrometer measurement of room air originally at 3.9 g/m^3 absolute humidity (19.4 % relative humidity, 22.6 °C) after being pulled through water permeation tube and inlet at various temperatures at 3.6 L/min.